Dynamic Deformation Behavior of Aluminum Alloys Under High Strain Rate Compressive/Tensile Loading

Ouk Sub Lee*, Guan Hee Kim, Myun Soo Kim
School of Mechanical Engineering, Inha University,
253 Yonghun-dong, Nam-gu, Incheon 402-751, Korea
Jai Sug Hwang
School of Mechanical Engineering, Yeungnam University,
214-1, Dae-dong, Gyeongsan-si, Gyeongsangbuk-do 712-749, Korea

Mechanical properties of the materials used for transportations and industrial machinery under high strain rate loading conditions such as seismic loading are required to provide appropriate safety assessment to these mechanical structures. The Split Hopkinson Pressure Bar (SHPB) technique with a special experimental apparatus can be used to obtain the material behavior under high strain rate loading conditions. In this paper, dynamic deformation behaviors of the aluminum alloys such as Al2024-T4, Al6061T-6 and Al7075-T6 under both high strain rate compressive and tensile loading conditions are determined using the SHPB technique.

Key Words: SHPB (Split Hopkinson Pressure Bar), Aluminum Alloys(Al2024-T4, Al6061-T6, Al7075-T6), Dynamic Stress-Strain Curve, Stress Wave, Deformation Behavior, High Strain Rate, Dynamic Maximum Compressive/Tensile Stresses, Spurious Wave, Seismic Loading

Nomenclature

L	: Specimen length
$\varepsilon_{specimen}$	: Specimen strain
$\sigma_{specimen}$	: Specimen stress
$\dot{\varepsilon}$	: Strain rate
E	: Young's Modulus
A	: Cross-sectional area of the bar
A_s	: Cross-sectional area of the specimen
C_0	: Longitudinal wave velocity
ε_I	: Incident strain
ε_R	: Reflected strain
ε_T	: Transmitted strain
R	: Radius of the bar

* Corresponding Author,
E-mail : leeos@inha.ac.kr
TEL : +82-32-860-7315; **FAX** : +82-32-860-1716
School of Mechanical Engineering, Inha University, 253 Yonghun-dong, Nam-gu, Incheon 402-751, Korea.
(Manuscript **Received** August 2, 2001; **Revised** January 30, 2003)

1. Introduction

The compressive and tensile tests under high strain rate loading should be distinguished from those of low strain rate. The effect of inertia is not negligible in the test under high strain rate loadings. The manifestation of inertia in a dynamic test is mainly threefold. First, it induces a radial component to the stress that may not be negligible in some conditions. Second, inertia is responsible for the heterogeneity of deformation present in the specimen at the beginning of the test. And third, inertia affects the elongation stability.

Recently, we may find many cases in that mechanical materials are being used under extreme conditions such as forging and rolling characterized by high stresses and high strain rate loading. In order to design structures used under extreme loading conditions, we need to know mec-

hanical deformation behaviors of the material under high strain rate in detail. It is not easy, however, to get the mechanical properties under the high strain rate loading condition.

A specific experimental method, the split Hopkinson pressure bar (SHPB) technique has been suggested to determine the dynamic material properties under the impact compressive and tensile loading conditions with strain-rate of the order of 10^3/s (Hopkinson, 1914). SHPB has been commonly used to obtain the high strain rate between 10^3/s and 10^4/s (Kang et al, 1997; Huh et al, 2002).

2. Theory

2.1 One-dimensional elastic wave propagation in a bar

Pochhanmmer and Chree solved the longitudinal and radial inertia effect (Pochhammer, 1876; Chree, 1889) on a specimen perfectly contacted with the bars in SHPB experiment. By this result, the specimen geometry in Hopkinson bar experiment could be designed to remove inertia effect. If the stress wave were a cosine wave of wavelength, λ, the longitudinal deformation and stress by the stress wave might be constant, when $R/\lambda \ll 1$ (Davies, 1948).

2.2 Uniform deformation of the specimen

It is difficult to analyze the deformation of a specimen due to the effects of plastic wave propagation and friction, while the elastic wave propagation in the bar may be expected. The influence of friction is reduced by spreading a viscous lubrication cream evenly. Even though the specimen deforms uniformly, errors may be generated by the longitudinal and radial inertia caused by the sudden particle acceleration in high strain rate.

2.3 The stress-strain rate determination by SHPB

2.3.1 Compressive test

In conventional SHPB technique, the specimen is located in between incident and transmitted bars. General compressive elastic wave propagation behavior in SHPB is shown in Fig. 1. When the striker bar impacts the incident bar, rectangular stress pulse is generated and travels along the incident bar until it hits the specimen. Part of the incident stress pulse reflects from the bar/specimen interface because of the material impedance mismatch, and part of it transmits through the specimen. The transmitted pulse emitted from the specimen travels along the transmitted bar until it hits the end of the bar. The stress, strain and strain rate in the specimen can be obtained in terms of the recorded strains of the two bars as follows (Follansbee, 1985).

$$\sigma_{specimen} = E\left(\frac{A}{A_s}\right)\varepsilon_T \tag{1}$$

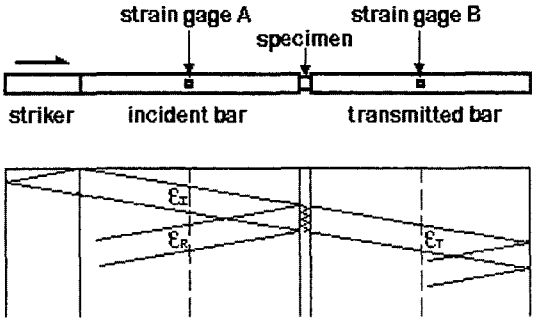

Fig. 1 A schematic diagram of specimen and elastic stress wave propagation for the compressive test

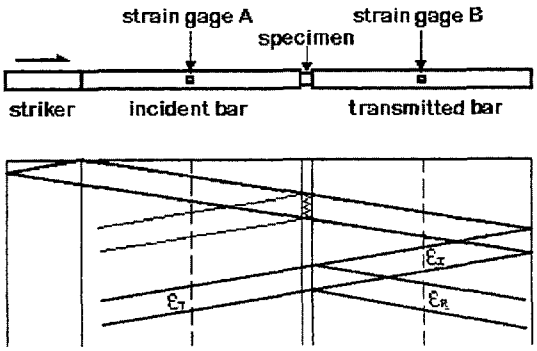

Fig. 2 A schematic diagram of specimen and elastic stress wave propagation for the tensile test

$$\varepsilon_{specimen}=\frac{\mp 2C_0}{L}\int \varepsilon_R dt \tag{2}$$

$$\dot{\varepsilon}_{specimen}=\frac{d\varepsilon(t)}{dt}=\frac{-2C_0}{L}\varepsilon_R(t) \tag{3}$$

2.3.2 Tensile test

In the tension test using SHPB technique, specimen is located in between incident and transmitted bars. General tensile elastic wave propagation behavior in SHPB is shown in Fig. 2.

The compressive stress pulse generated in the incident bar by the impact of striker bar travels along the specimen and the split ring (see Fig. 4). The compressive stress pulse propagates until it arrives the end of the transmitted bar. The compressive stress pulse arrived the end of the transmitted bar reflects by the shape of tensile stress pulse. The tensile stress pulse is recorded at strain gage B. Part of tensile stress pulse reached at the specimen propagates to the incident bar, and the rest of the wave reflects to the transmitted bar. It is important to locate the strain gages where no interference between the tensile stress wave (ε_T) and the spurious wave generated at the incident bar/split ring interface. The spurious wave has bad effect on the results because it applies pretension to the specimen. But this phenomenon is unavoidable in high strain rate tests. The split ring located between incident bar and transmitted bar has no effects on the tensile loading because it does not mechanically jointed to the two bars. The snug fit between split ring and incident and transmitted bars is important to keep one-dimensional wave propagation condition.

3. Experiment

3.1 Loading apparatus and striker bar

In this study, the incident, transmitted and striker bars are made of STB2 whose yield strength is 490 MPa and the modulus of elasticity is 225 Gpa, SHPB apparatus used for this study is shown in Photo 1.

The length and the diameter of the striker are 300 mm and 16 mm, respectively. The diameters of incident bar and transmitted bar have the same dimension as the striker bar.

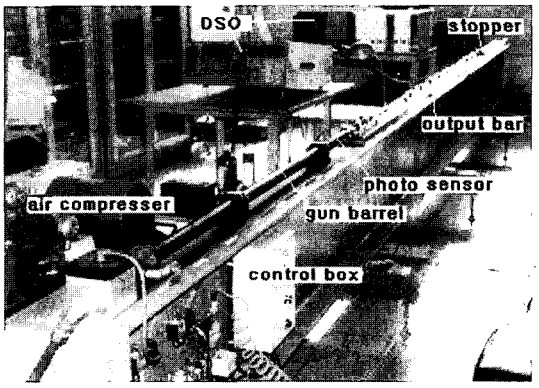

Photo. 1 experimental setupeke

3.2 Incident and transmitted bars

3.2.1 Compressive test

The smaller the diameter of the pressure bars, the higher strain rate in the specimen will be gained. The bar length has to be twice of wavelength of stress pulse in the bars, so the ratio of the length to the diameter of the bars was designed to be 100. These two bars are made of the same material of striker bar and have the identical diameter with striker bar. To obtain perfect contact of the incident and the transmitted bar surfaces, the ends of the bars are finely grinded (Lee et al, 1998 ; Lee et al, 2000 ; Lee et al, 2000).

3.2.2 Tensile test

The incident bar and transmitted bar are screwed to fix the specimen in them. When we set the specimen into the incident and transmitted bars, we turn the specimen in one direction. So one of the bars is machined right-hand screw and the other is left-hand screw. The cross-sections are heat treated to prevent deformation by continuous impacts.

3.3 Straight-line guider and stopper

One of the most important things of the apparatus is the straight-line guide so that the stress pulse can propagate in one dimension. After fine grinding an I-beam, the bar is setup on the beam

by using the fine bearing system.

3.4 Velocity and wave measurement system

To measure the velocity, three photo sensors are located at the distance of 50 mm in the end of the gun barrel. When the striker cuts the light of the photo sensors, and oscilloscope, Nicolet 410, gets electric signals. By the strain gages bonded on the middle of the bars, the stress pulse can be obtained.

3.5 Specimen preparation

3.5.1 Compressive

The geometry of specimen should meet the condition to minimize the effect of inertia. So the specimens used for this study have 5mm thickness and 10 mm diameter. The geometry of specimen is shown in Fig. 3.

3.5.2 Tensile

The whole length, diameter and gage length of specimen is 34 mm, 4 mm and 12 mm, respectively. The both ends of specimen manufacture in a screw shape in order to be fixed in incident and transmitted bars (Lee et al, 2000; Bragov, 1994).

The ratio of cross-sectional area of split ring to pressure bar cross-sectional area is the three to four. The ratio of cross-sectional area of split ring to specimen cross-sectional area is twelve to one. Geometry of split ring and collar is shown in Fig. 4.

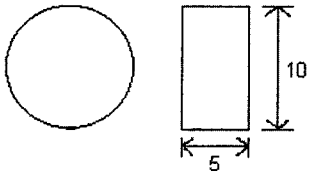

Fig. 3 Geometry of compressive specimen

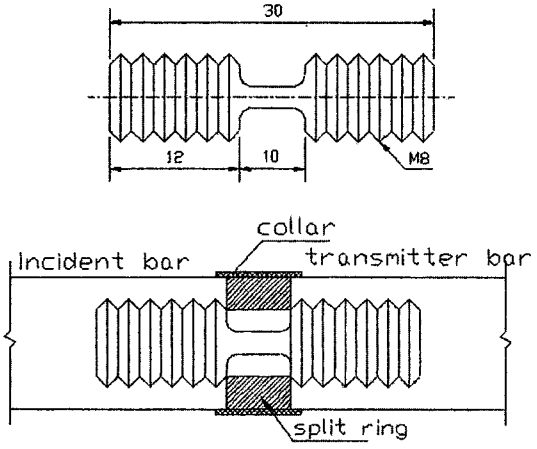

Fig. 4 Specimen geometry and setting between incident and transmitted bar (dimension=mm)

4. Results and Discussion

The typical compressive and tensile signal outputs form strain gages attached on incident and transmitted bars, respectively, are shown in Fig. 5. It is noted that the superposed wave of the ref-

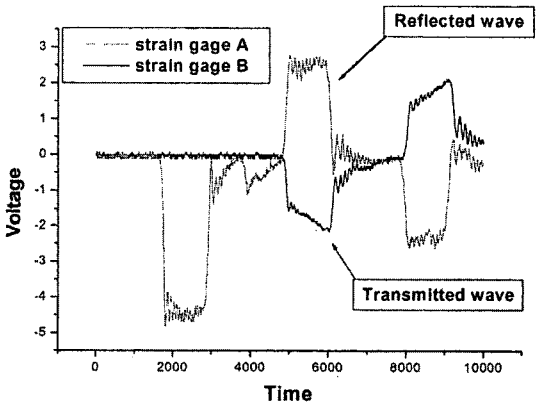

Fig. 5(a) Strain signal recorded at oscilloscope (compressive)

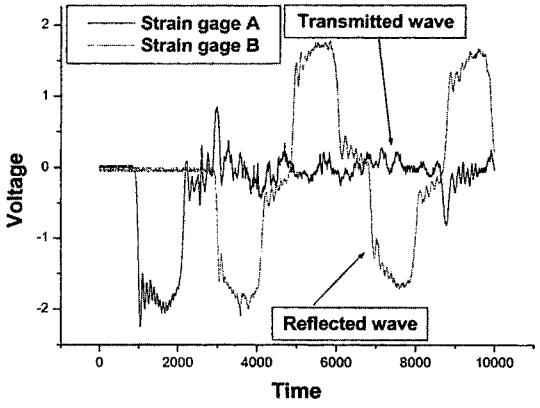

Fig. 5(b) Strain signal recorded at oscilloscope (tensile)

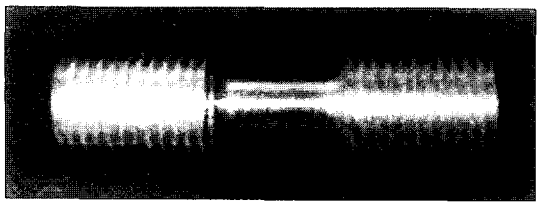

Photo. 2 Aluminum specimen before dynamic tensile test

Photo. 3 Aluminum specimen after dynamic tensile test

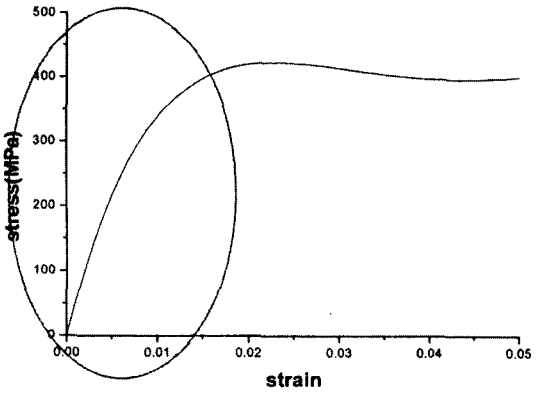

Fig. 6(a) Compressive stress-strain curve for 2024-T4

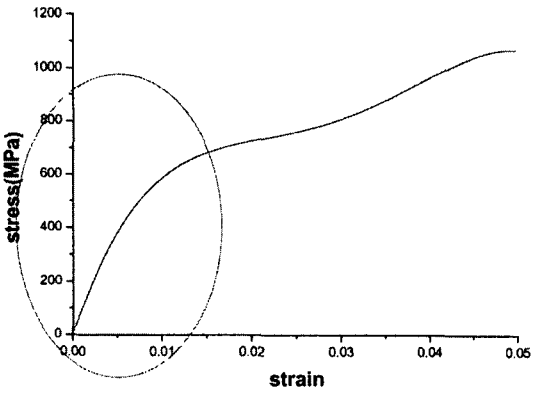

Fig. 6(b) Tensile stress-strain curve for 2024-T4

lected and transmitted wave are almost the same as the incident waves.

Photos 2 and 3 shows the specimen configuration before and after the test, respectively.

It is interesting to note that the cup and cone fracture is clearly distinguished.

Using Eqs. (1) and (2), the relationship between stress and strain under high strain rate compressive and tensile loading conditions can be obtained. Fig. 6 shows the typical dynamic compressive and tensile stress-strain behavior up to strain of 0.05 for Al2024-T4. We have noted in this paper the initial range of the whole stress-strain curve as marked by an elliptical portion shown in Fig. 6 since the first yielding occurred in this region. (Zukas, 1990) The typical results of initial range of the whole stress-strain curve and numerical modelings for various aluminum alloys are shown in Fig. 7. The effects of strain rate on the relationships of stress-strain for varying aluminum alloys are found to be pronounced for both compressive and tensile loading cases. Furthermore, it is noted that the general mechanical deformation behaviors under high strain rate of compressive and tensile loading conditions are quite different from each other as shown in Fig. 7.

A polynomial best fitting is utilized to model the dynamic stress-strain behavior in case for a numerical simulation such as the finite element method.

Table 1(a) Coefficients of the fourth order polynomials for compressive test

$\sigma=a+b_1\varepsilon^1+b_2\varepsilon^2+b_3\varepsilon^3+b_4\varepsilon^4$					
Materials	a	b_1	b_2	b_3	b_4
2024-T4	0	5.66×10^4	-1.63×10^6	-3.10×10^7	1.25×10^9
6061-T6	0	9.38×10^4	8.09×10^6	2.97×10^8	-4.01×10^9
7075-T6	0	3.07×10^4	4.08×10^6	-2.61×10^8	3.62×10^9

Table 1(b) Coefficients of the third order polynomials for tensile test

$\sigma=a+b_1\varepsilon^1+b_2\varepsilon^2+b_3\varepsilon^3+b_4\varepsilon^4$					
Materials	a	b_1	b_2	b_3	b_4
2024-T4	0	2.50×10^7	-2.05×10^8	7.46×10^8	-1.01×10^9
6061-T6	0	1.57×10^8	-1.37×10^9	5.32×10^9	-7.73×10^9
7075-T6	0	74862.36	-4.06×10^6	1.01×10^8	-8.05×10^8

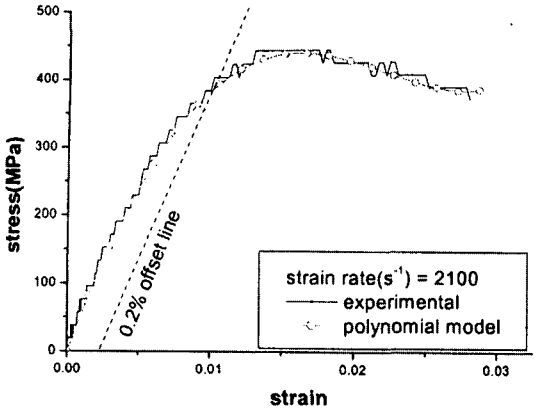

Fig. 7(a) Experimental and polynomial model of dynamic compressive stress-strain curve for Al2024-T4

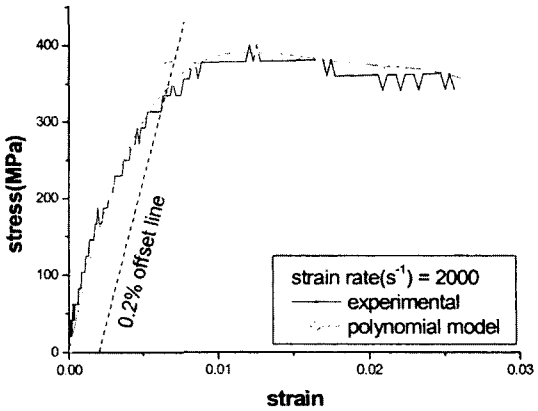

Fig. 7(b) Experimental and polynomial model of dynamic compressive stress-strain curve for Al6061-T6

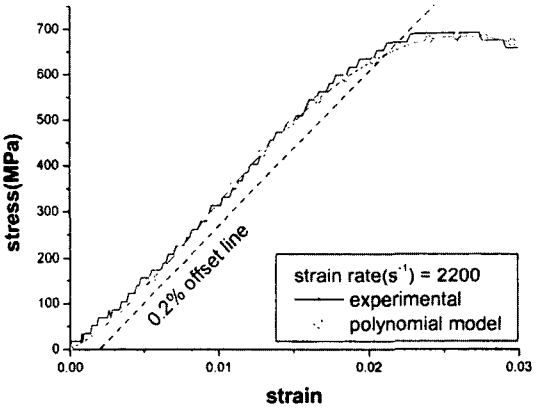

Fig. 7(c) Experimental and polynomial model of dynamic compressive stress-strain curve for Al7075-T6

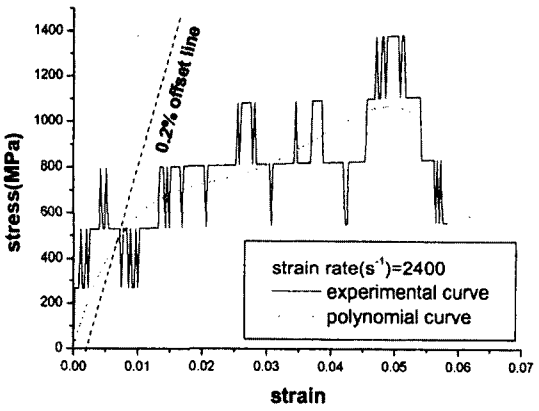

Fig. 7(d) Experimental and polynomial model of dynamic tensile stress-strain curve for Al2024-T4

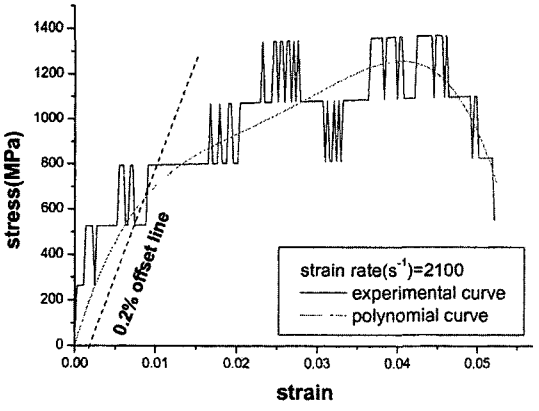

Fig. 7(e) Experimental and polynomial model of dynamic tensile stress-strain curve for Al6061-T6

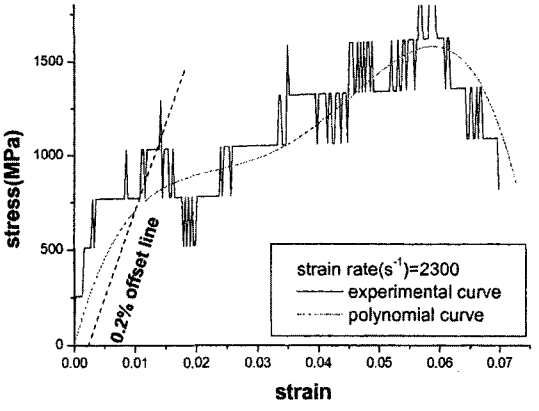

Fig. 7(f) Experimental and polynomial model of dynamic tensile stress-strain curve for Al7075-T6

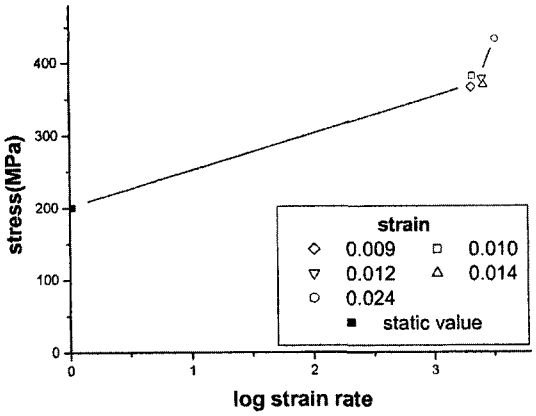

Fig. 8(a) Dynamic log strain rate versus compressive yield stress for Al2024-T4

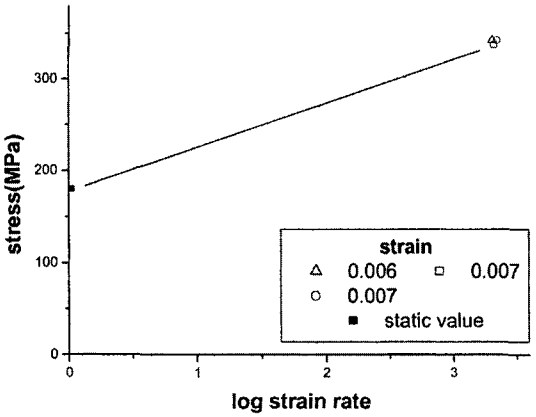

Fig. 8(b) Dynamic log strain rate versus compressive yield stress for Al6061-T6

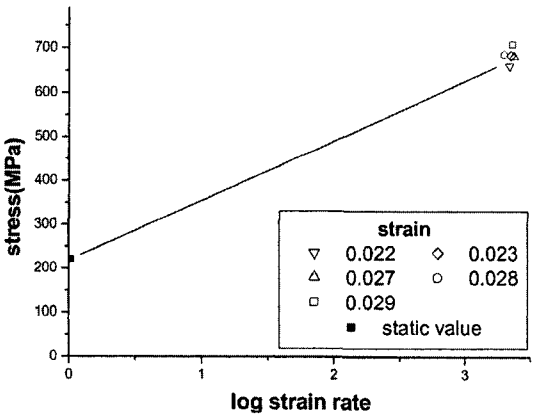

Fig. 8(c) Dynamic log strain rate versus compressive yield stress for Al7075-T6

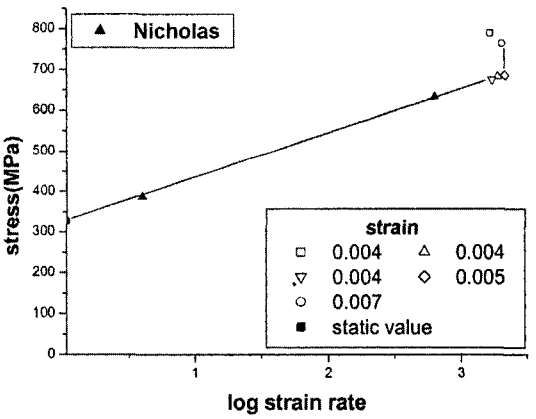

Fig. 8(d) Dynamic log strain rate versus tensile yield stress for Al2024-T4

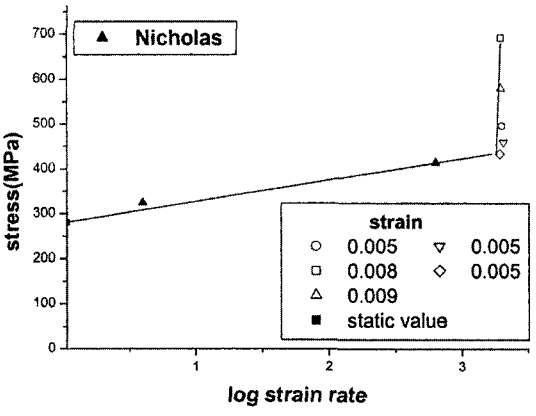

Fig. 8(e) Dynamic log strain rate versus tensile yield stress for Al6061-T6

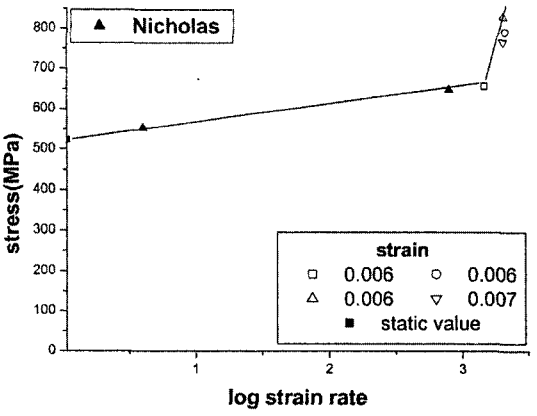

Fig. 8(f) Dynamic log strain rate versus tensile yield stress for Al7075-T6

The fourth order polynomials are found to be the best appropriate models for compressive and tensile, respectively, to represent the relationships between dynamic stresses and dynamic strains under high strain rate loading conditions. The coefficients of the third and fourth order polynomials for varying aluminum materials are listed in Table 1.

The yield stresses are estimated by drawing a 0.2% offset line to the best representative slope as indicated in Fig. 7. It is found that the relationships between yield stresses and strain rates are quite different from each other corresponding to compressive and tensile loading conditions.

However, it was speculated that these phenomena are originated from the different experimental set ups as noted in section 3. We further speculated that such phenomena represented the material characteristics under different loading conditions for tested aluminum alloys. We need to investigate this point of view further in detail in near future.

Figs. 8 shows the relationship between yield stresses determined by using a procedure suggested in this study and strain rates.

The results by Nicholas (Nicholas, 1981) are included in Figs. 8(d), (e) and (f). It is very interesting to note that Nicholas' results are well agreed with the results estimated in this paper.

The sensitivity which may be defined as $\{(\sigma_{dyn}-\sigma_{stat})/\sigma_{stat}\}$ for tensile strength of Al2024-T4, Al6061-T6 and Al7075-T6 are found to be more sensitive than compressive strength. And, it is also found that compressive yield strength of Al2024-T4 and tensile yield strength of Al2024T-4, Al7075-T6 and Al 6061-T6 under high strain-rate loading increased in bilinear in the semi-logarithmic coordinate system.

5. Conclusion

The dynamic deformation behaviors of Al2024-T4, Al6061-T6 and Al7075-T6 under both compressive and tensile loading conditions are estimated by using SHPB techniques and the following experimental results are obtained.

(1) The relationships between compressive yield strength and strain rate for Al6061-T6 and Al7075-T6 are linear while the relationships between tensile yield strength and strain rate of Al2024-T4, Al6061-T6 and Al 7075-T6 and the relationships between compressive yield strength and strain rate of Al2024-T4 are bilinear in the semi-logarithmic coordinate system.

(2) The sensitivity $\{=(\sigma_{dyn}-\sigma_{stat})/\sigma_{stat}\}$ of Al2024-T4, Al6061-T6 and Al7075-T6 are found to be 93%, 89% and 211% at compressive yield strength and 120%, 90%, 45% at tensile yield strength, respectively.

Acknowledgment

This research is supported by 2001 Korea Research Foundation (E00061).

References

Bragow, A. M. and Lomunow, 1994. "Methodological Aspects of Studying Dynamic Material Properties Using the Kolsky Method," *Int. J. Impact Energy*, Vol. 16, pp. 321～330.

Chree, C., 1889, "The Equations of an Isotropic Elastic Solid in Polar and Cylindrical Coordinates," *Their Solutions and Applications, Cambridge Phil. Soc. Trans.* Vol 14, p. 250.

Davies, R. M., 1948, "An Critical Study of the Hopkinson Pressure Bar," *Phil. Tran. A*, Vol. 240, p. 375.

Follansbee, P. S., 1985, "〈The Hopkinson Bar〉, in Metals Handbook Ninth Edition, Mechanical Testing," *American Society for Metals*, Vol. 8, pp. 198～203.

Hopkinson, B., 1941, "A Method of Measuring the Pressure Produced in the Detonation of Explosives or by the Impact of Bullets," *Phil. Trans. A*, Vol. 213, p. 437.

Huh, H., Kang, W. J. and Han, S. S., 2002, "A Tension Split Hopkinson Bar for Investigating the Dynamic Behavior of Sheet Metals," *SEM International Journal*, Vol. 42, No. 1, pp. 8～17.

Kang, W. J., Cho, S. S., Huh, H. and Chung, D, T., 1997, "High Strain-rate Tensile Test of Sheet Metals with a New Tension Split Hopkinson

Bar," *Trans. KSME*, Vol. 21, No. 12, pp. 2209~2219.

Lee, O. S., Lee, S. S., Chung, J. H. and Kang, H. S., 1998, "Dynamic Deformation Under Bar Experiment," *KSME International Journal*, Vol. 12, No. 6, pp. 1143~1149.

Lee, O. S., Lee, J. Y., Kim, G. H. and Hwang, H. S., 2000, "High Strain-rate Deformation of Composite Materials Using a Split Hopkinson Bar Technique, Key Engineering Materials," 183~187, Part 1, pp. 307~312.

Lee, O. S. and Kim, G. H., 2000, "Thickness Effects on Mechanical Behavior of a Composite Material (1001P) and Polycarbonate in Split Hopkinson Pressure Bar Technique," *Journal of Materials Science Letters*, Vol. 19, pp. 1805~1808.

Lee, O. S. and Kim. G. H., 2000, "Determination of Deformation Behavior of the Al6061-T6 under High Strain Rate Tensile Loading Using SHPB Technique," *Transaction of KSME (A)*, Vol. 24, No. 12, pp. 3033~3039 (in Korean).

Nicholas, Theodore, 1981, "Tensile Testing of Materials at High Rates of Strain," *Experimental Mechanics*, Vol. 21, pp. 177~185.

Pochhammer, L., 1876, "On the Propagation Velocities of Small Oscillations in an Unlimited Isotropic Circular Cylinder," *J. Reine Angewandte Math*, Vol. 81, p. 324.

Zukas, J. A., 1990, "High Velocity Impact Dynamics," John Wiley & Sons, Inc.